Molecular Properties and Chemical Transformations Near Interfaces

Musahid Ahmed, Monika Blum, Ethan J. Crumlin, Phillip L. Geissler, Teresa Head-Gordon*, David T. Limmer, Kranthi K. Mandadapu, Richard J. Saykally, Kevin R. Wilson

Chemical Sciences Division, Lawrence Berkeley National Laboratory, Berkeley, CA 94720

The properties of bulk water and aqueous solutions are known to change in the vicinity of an interface and/or in a confined environment, including the thermodynamics of ion selectivity at interfaces, transition states and pathways of chemical reactions, and nucleation events and phase growth. Here we describe joint progress in identifying unifying concepts about how air, liquid, and solid interfaces can alter molecular properties and chemical reactivity compared to bulk water and multi-component solutions. We also discuss progress made in interfacial chemistry through advancements in new theory, molecular simulation, and experiments.

*corresponding author: thg@berkeley.edu

Musahid Ahmed is a senior scientist at Lawrence Berkeley National Labs, Berkeley, USA. He received his PhD in 1989 at Cambridge University and then went on to perform postdoctoral work in Leicester,

Göttingen, and Manchester. Probing gas, interfacial and condensed phase chemical dynamics with X-ray, VUV, IR and THz radiation is his passion.

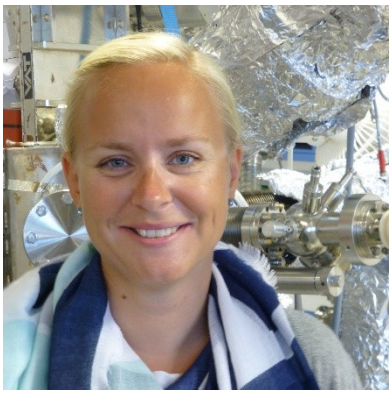

Monika Blum is a research scientist at the Advanced Light Source and the Chemical Sciences Division at Lawrence Berkeley National Lab, Berkeley, USA. She received her Diploma in Nano Science (2006) and PhD in Physics (2009) in the Department of Experimental Physics II at the University of Würzburg, Germany and went on to perform postdoctoral work at the University of Nevada, Las Vegas and LBNL (2009) before working in industry. She uses X-ray emission, X-ray absorption, and RIXS as well as ambient-pressure XPS to characterize energy materials and solid-gas, solid-liquid, and liquid-liquid interfaces.

Ethan J. Crumlin is a Career Staff Scientist at the Advanced Light Source at Lawrence Berkeley National Laboratory. He received his B.S. (2005), M.S. (2007), and Ph.D. (2012) in the Department of Mechanical Engineering from MIT, and became a Postdoctoral Fellow at LBNL (2014). He leads a research group to use ambient pressure X-ray photoelectron spectroscopy (APXPS) to study chemical and electrochemical reactions at the solid-gas, solid-liquid, and solid-solid interfaces for fuel cell, catalysts, battery, and other electrochemical systems.

Phillip Geissler is a Professor of Chemistry at University of California Berkeley and a Faculty scientist at Lawrence Berkeley National Laboratory. He received his Ph.D. from UC Berkeley (2000), was a postdoctoral scholar at Harvard (2001), and held a Science Fellowship at MIT (2001-2003). His research develops and applies theoretical tools of statistical mechanics to understand microscopic fluctuations of complex molecular systems, with an emphasis on aqueous interfaces, biological self-assembly, and nano-scale materials.

Teresa Head-Gordon is a Professor of Chemistry, Bioengineering, and Chemical and Biomolecular Engineering at University of California Berkeley and a Faculty scientist at Lawrence Berkeley National Laboratory. She received her Ph.D. from Carnegie Mellon University (1989) and was a Postdoctoral Member of Technical Staff at AT&T Bell Laboratories (1990-1992). Her independent career began as Scientist at Lawrence Berkeley National Laboratory (1992-2000) and she joined the UC Berkeley faculty in 2001. She has an abiding interest

in the development and application of theoretical models and computational methods that are widely disseminated through many community software codes, with applications to materials, biophysics, catalysis, and interfacial reactivity.

David Limmer is an Assistant Professor of Chemistry at the University of California Berkeley, a Faculty Scientist at Lawrence Berkeley National Laboratory, and a Fellow of the Kavli Energy NanoSciences Institute. He received his Ph.D. in chemistry from the University of California, Berkeley under the supervision of David Chandler, and was an independent fellow of the Princeton Center for Theoretical Science (2013-2016). His research endeavors to advance theoretical descriptions of complex, condensed phase materials especially in instances where equilibrium ideas do not apply. Specific areas of current interest include the emergent behavior of systems undergoing simple chemical dynamics in complex environments and nanoscale systems driven far from equilibrium.

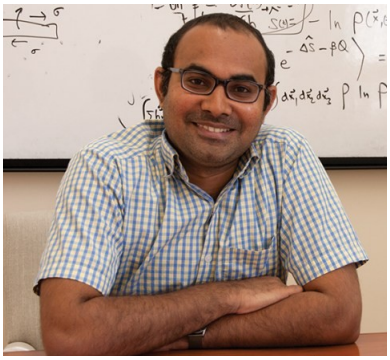

Kranthi Mandadapu is an Assistant Professor of Chemical and Biomolecular Engineering at the University of California Berkeley and a Faculty scientist at Lawrence Berkeley National Laboratory. He received his Ph.D. in mechanical engineering from the UC Berkeley, and was a postdoctoral fellow under the supervision of David Chandler. He is broadly interested in understanding how materials behave at multiple length and time scales using approaches at the intersection of statistical mechanics, continuum mechanics (fluid and solid mechanics), and applied mathematics. He work with problems in the field of physics of soft and living systems including biological membranes, active matter, polycrystalline and amorphous systems.

Richard Saykally is the Class of 1932 Endowed Professor of Chemistry at UC Berkeley and a Faculty scientist at Lawrence Berkeley National Laboratory. He is coauthor of over 400 publications that have been cited over 50,000 times (h-index >100), and he is the recipient of over 75 honors and awards from 15 different countries.

Kevin Wilson is a senior scientist and the Deputy Director of the Chemical Sciences Division at Lawrence Berkeley National Laboratory. He earned a Ph.D. from the University of California, Berkeley in 2003, and received a Fredrick Reines Distinguished Postdoctoral Fellowship from Los Alamos National Laboratory (2003-2004). His research group uses novel mass spectrometry methods,

kinetic modeling and synchrotron-based spectroscopy to elucidate heterogeneous reactions mechanisms in aerosols and droplets.

1. INTRODUCTION

Chemistry rarely occurs in a homogeneous aqueous phase, but instead occurs inside niches, within crevices, between surfaces, and at impurity sites involving interfaces between two or more phases of gases, liquids or solids. Interfacial induced changes of molecular properties feeds up at an operational level to a diverse range of chemical, biophysical, and applied environmental[1] and energy systems including[2]: the membrane pores for chemical separations and 2D crystals[3] used for clean water generation[4]; nanoconfinement chemistry[5], soft matter self-assembly[6], complex interfaces for heterogeneous catalysis for targeted energy reactions[7], intergranular corrosion in metals[8], aerosol and atmospheric particles[9-10], and reaction rate acceleration in nanodroplets[11] and microdroplets[12], However, at present we lack the ability to accurately predict most molecular processes in such systems because interfacial and confinement effects violate our understanding of these same processes gained from bulk phase studies. In particular, when the correlation lengths in space and/or time of the interfacial system become comparable to that of a given molecular property, how that property is altered will now depend sensitively on the specifics of the interfacial geometry and chemistry. In this Perspective our team seeks to unify the aspects of interfacial features that are predictive for functional outcomes by a systematic strategy of changing the nature of the interface from a prototypical air-water interface[13-14], and then expanding into more complex condensed phase environments.

The structural organization and thermodynamics of ion solvation as well as ice nucleation and growth[15] under complex environments are demonstrably different from the bulk phase. In many real-world applications the active role that water ubiquitously plays in interfacial chemistry[16] also is an important theme as we contrast air-water vs. solid-water interfaces to better reveal how key structural motifs change the thermodynamic behavior of ion solvation at the gas vs. solid interface.[17-18] With careful studies of ice nucleation in the bulk[19], we contrast nucleation and growth properties of water under confinement between graphene sheets[20] or at grain boundaries[21] which has important implications for chemical reactions on ice[22-25] and gaseous SO_2 uptake in ice[26].

We also discuss the elucidation of the principles that control reactivity in heterogeneous environments where interfacial processes are inextricably connected to chemical transformations such as “on-water” chemistry and other types of fundamental organic reactions that have been

found to be catalyzed by microdroplet interfaces.[27-28] Classic organic reactions such as retro-Diels-Alder help to elucidate the effects of nano-confinement on solvent properties and their effects on reactivity[29], as well as the diffusive and mesoscale confinement in droplets and aerosols that can alter overall reaction rates and mechanisms.[30-31] Heterogeneous catalysis and electrocatalysis enables important chemical reactions that are thermodynamically uphill, such as the splitting of water to produce H_2 and the reduction of CO_2 to fuels, to be carried out at ambient conditions. These interfaces under *in situ* conditions restructure[32] and drive chemical transformations through multiple intermediates[33], and poses a remarkable series of challenges for theory and computation to elucidate the sequence of events at the molecular scale[34-36].

We highlight the theoretical and experimental advances that have enabled our team to tackle systems that are heterogeneous and profoundly complex in composition. There is a substantial experimental gap in methods that can achieve microsecond and sub-microsecond mixing times, critical timescales for observing reactive intermediates (such as radicals) in condensed phase reactions, and requiring an integrated spectroscopy platform with a colliding droplet reactor to probe fast events.[37] In addition to seminal work of using soft X-Rays coupled to liquid jets,[38] the recently developed Velocity Map Imaging (VMI)[39] method uses X-Ray photoelectron spectroscopy to probe aerosols and nanoparticles.[40-41] Ambient Pressure XPS (APXPS) with soft (<2 keV) and tender X-rays (2 keV to 6 keV)[33, 42-46] has enabled the ability to probe solid-liquid interfaces and ideal for buried interfaces between 10's of nm thick liquid electrolytes. We have developed new theoretical approaches for understanding the non-equilibrium dynamics in clays[47] and confined aqueous systems[48], the transport properties and phase behavior of glasses[49], and the self-assembly of amphiphilic structures[50]. Finally, we summarize our Perspective with new experimental and theoretical efforts that will be needed to more seamlessly connect structure and dynamics that cross disparate scales in order to better understand emergent phenomena for interfacial systems in the future.

2. ION SOLVATION AT INTERFACES

Water's ability to favorably solvate ions and polar molecules, and its inability to accommodate large nonpolar species, underlies many of its essential roles in shaping reactivities central to energy sciences and biophysics. A century of quantitative measurements, theoretical

development, and modeling efforts have established a basic mechanistic view of aqueous solvation and many tools to explore its molecular underpinnings and chemical implications. Molecular dynamics simulations can, for instance, describe bulk ion solvation free energies with good to excellent accuracy[51], provided a careful treatment of long-ranged electrostatic forces via Ewald summation conducted under periodic boundary conditions. This approach has been extremely reliable for structural, thermodynamic, and transport properties, once finite size corrections are applied.[52]

In many ways, however, our understanding of ion solvation remains markedly incomplete. Dielectric continuum theory (DCT), which embodies the classic physical perspective on charged solutes in polar solvents, fails to capture large thermodynamic distinctions between the solvation of positively and negatively charged ions that are otherwise identical. Spatially heterogeneous environments compound these shortcomings significantly, bringing into play modes of solvent response that can be neglected in the symmetric environment of a bulk liquid. Key interfacial behaviors, such as the surface enhancement of some anions and the exclusion of corresponding cations,[53] lack a thorough understanding as a result, and a general theory for ion solvation at surfaces is still wanting. Surface-specific spectroscopies that might clarify the situation are both challenging to perform precisely and notoriously difficult to interpret reliably in microscopic terms.

To help address this gap, Geissler and Saykally have studied the adsorption of prototypical anions to the air-water interface by using the surface-selective method of second harmonic generation spectroscopy (SHG) along with computer simulations. By measuring SHG intensities as a function of bulk ion concentrations, simple Langmuir adsorption models yield the Gibbs free energy of adsorption, whose temperature dependence permits separation into enthalpic and entropic contributions. For the thiocyanate anion (SCN^-), a prototypical chaotrope, surface adsorption is unexpectedly favorable enthalpically, which can be ascribed to a repartitioning of solvent molecules among bulk, interfacial, and ion hydration shell environments. Also surprising is a positive entropy of adsorption, which is suggestively accompanied by a suppression of fluctuations in interfacial shape.[17] As a route to further clarifying the mechanism that selectively drives ions to and away from the air/water interface, the Saykally group have developed a new experiment (Deep UV Sum Frequency Generation) for

measuring the complete charge transfer to solvent (CTTS) spectrum of interfacial anions, and have applied it to the prototypical cases of SCN^- and the iodide anion.[54] The spectra show significant differences from the bulk CTTS spectra, and provides a new variable for constructing general theoretical models to explain interfacial ion behavior.

Geissler and Saykally have tested the generality of their mechanistic picture for ion adsorption at the air-water interface by examining solvation in a different interfacial context, namely liquid water in contact with graphene. Deep UV Second Harmonic Generation (SHG) measurements of the SCN− ion determined a free energy of adsorption at graphene within experimental error of that determined for air/water, in accord with the findings from molecular simulations that model anions absorb almost equally strongly at these two interfaces.[18] Interestingly however, computer simulations indicate that the enthalpic and entropic components of the adsorption free energy differ significantly in the two cases (Fig. 1). Whereas the adsorption energy at the air/water interface is dictated by repartitioning of solvent molecules, direct interactions between the ion and graphene are dominant in the case of graphene/water. Moreover, interface shape fluctuations are suppressed by graphene even in the ion's absence, so that the entropic consequences of capillary wave pinning by the ion are attenuated considerably.

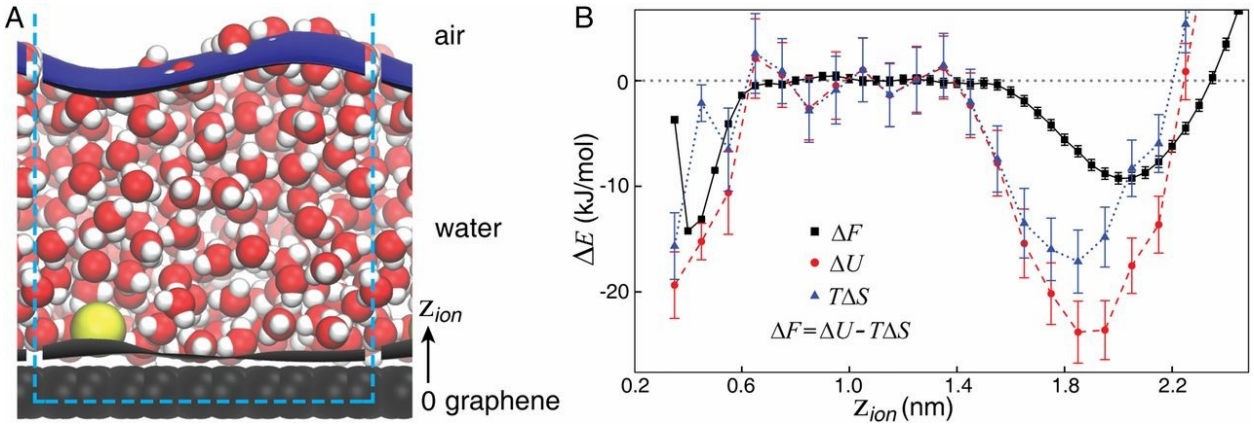

Figure 1. *Solvation of a model ion at the interface between liquid water and graphene*. (A) Snapshot from a molecular dynamics simulation, with the air/water (upper) and graphene/water (lower) interfaces rendered as smooth surfaces identified from a coarse-graining of the microscopic density field. Note the substantial suppression of capillary fluctuations at the lower interface. (B) Profiles of key thermodynamic quantities as functions of the solute's distance z relative from the graphene sheet, computed by umbrella sampling. Features at small and large z highlight differences in solvation at the two interfaces. The entropy profile is nearly constant at small z (aside from a drop at the leftmost point, where the solute begins to clash sterically with the graphene sheet), consistent with a reduced significance of interfacial shape fluctuations. Used with permission from [18] under copyright 2017 National Academy of Sciences.

Because long-range electrostatic forces figure prominently in aqueous solvation, quantifying ion adsorption thermodynamics in computer simulations requires careful consideration of finite size effects. To extrapolate from the nanometer simulation scale l_{sim}, one can presume that a macroscopic description like DCT applies on all larger scales. In the case of solvation in bulk liquid water, this strategy yields a simple yet accurate finite size correction. Geissler and coworkers derived an analogous correction for the interfacial case, obtaining similarly close agreement with observed system size dependence.[55] In addition to providing a practical computational tool, successful extrapolation from small simulations (l_{sim} ~ 1nm) highlights the realism of DCT on scales larger than 1-2 molecular diameters, even for heterogeneous systems. Failures of DCT for predicting aqueous response on smaller scales indicates inappropriate omission of short-ranged physical features of water. Geissler and Mandadapu have recently shown that molecular quadrupole contributions can indeed largely account for errors in predicted ion solvation free energies, and have suggested an elaboration of DCT that accounts implicitly for the geometric relationship between water's dipole and quadrupole moments.[56]

3. ICE NUCLEATION AT INTERFACES

While effective control of ice nucleation under different environmental conditions is highly desirable[57-60], in reality it has proven to be incredibly challenging. This is partly because water does not usually freeze at its equilibrium melting point but can exhibit significant supercooling[61-63], and the resulting metastability[64-65] makes it difficult to control the ice nucleation event at the desired temperature. Previous work has shown that static electric fields have been effective in controlling ice nucleation without the need for nucleating agents, but the highest freezing temperature (T_f) of water that can be achieved in an electric field (E) was still uncertain until recently when Ahmed and co-workers performed a systematic study of the effect of an electric field on water freezing (Fig. 2).[19]

By varying the thickness of a dielectric layer and the voltage across it in an electro-wetting system, they showed that T_f increases sharply with increasing E – but only to a point (Fig. 2A). Using classical heterogeneous nucleation theory, they found that this behavior is due to saturation in the contact angle of the ice embryo with the underlying substrate, a saturation that

occurs at -3.5 °C after a critical value E of 6×10^6 V/m is reached. They also showed that it is possible to overcome this freezing saturation by controlling the uniformity of the electric field with carbon nanotubes (Fig. 2B)[19], in which they achieved a T_f of -0.6 °C using a larger field strength of E of 3×10^7 V/m. In this case a solid-liquid interface alters the mechanism due to changes in electric fields that are not uniform which they hypothesize leads to enhancement of ice nucleation (Fig. 2C).

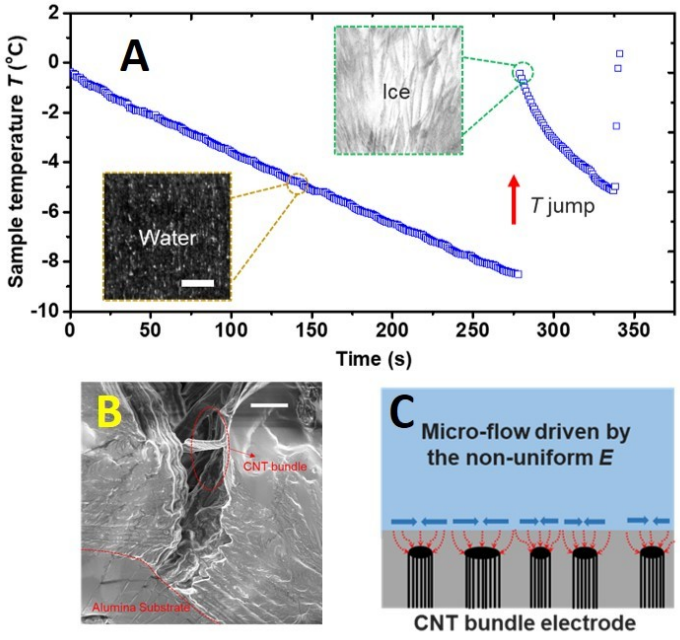

Figure 2. *Temperature-time curve showing the onset of freezing*. (A) The temperature of water was decreased linearly at the rate of 2 K min^{-1} until there was by a sudden temperature jump to 0 °C due to the release of latent heat. Inset shows pictures of the sample in liquid and solid phase during the experiment. The scale bar is 2 mm. (B) A scanning electron microscopy picture shows the carbon nanotube bundles on the alumina substrate, circled by dash line. The scale bar is 30 μm. (C) Also shown is a micro-scale mechanisms on the surface of a carbon nanotube inserted in water. The electric field strength is not uniform at the solid-liquid interface, which may cause micro-flow near the surface and facilitate ice nucleation. Adapted with permission from [19] Copyright 2020 American Chemical Society.

While bulk water freezes at low temperatures, and depending on pressure, into different ice phases, water at interfaces can exhibit a far richer phase diagram and phase-coexistence depending on experimental parameters. Real world experiments prepare and characterize nanoconfined water by employing interfaces that are inherently flexible and using irreversible kinetically controlled processes such as capillary compression or epoxy encapsulation so that the water content in the system is fixed. While most computational studies have focused on water confined within carbon nanotubes or between graphene sheets, the model hydrophobic confining surfaces are almost always rigid and the processes are assumed to be at equilibrium.

By lifting these two idealized conditions, the Head-Gordon lab showed that the nanoconfinement at fixed water densities were dramatically different when graphene was treated

as a rigid interface vs that of a highly flexible two-dimensional carbon allotrope.[20] While the rigid slit nanocapillaries exhibit sharp differences in the confinement distances at the transition between an (n)-layer and an (n+1)-layer water states, the flexible graphene walls allow the nanoconfined water to spatially split into an (n)-layer and an (n+1)-layer coexisting states (Fig. 3). Furthermore, the flexible walls introduce a very different sequence of ice phases and phase co-existence with vapor and liquid phases than that observed with rigid walls, with evident boundaries between square ice (as seen experimentally[66-67]), vapor, and liquid states. The flexible confining sheets also induce small patches of hexagonal ice that nucleate and dissipate on the time scales of the simulation, suggesting that water is close to a solid-liquid phase transition. This leads to many new questions about crystallization kinetics and how one can control aqueous based nucleation events at interfacial boundaries and use of confinement.

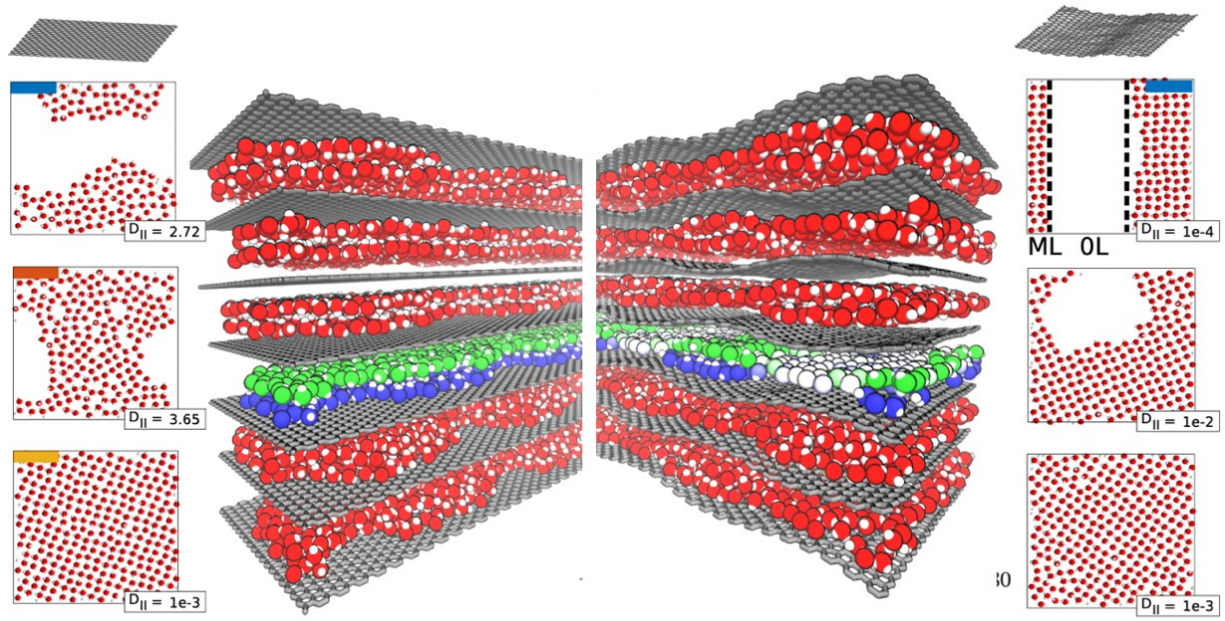

Figure 3. *Differences in water phases nanoconfined between rigid (left) and flexible (right) graphene surfaces.* While water adopts a bilayer structure (blue and green) for rigid surfaces, for flexible surfaces, monolayer (white) and bilayer (blue and green) water coexist within same interlayer. Adapted with permission from [20] copyright 2017 American Chemical Society

Mandadapu et al. have been focusing on the dynamics of supercooled liquids and solids, particularly formation of polycrystalline solids, which consists of single crystals oriented in different directions and solid-solid interfaces called grain boundaries. To this end, most materials, including water, capable of forming polycrystals can also form glasses or amorphous

solids. Whether a polycrystal or glassy structure is formed depends on the protocol or method by which the material is prepared such as the cooling rate or the annealing schedule. The resulting microstructure is a complex process involving competition between crystallization and vitrification, where the size of the crystals and resulting dynamics of the grain boundaries in polycrystals depend on the aforementioned formation protocols. Slower cooling rates produce larger grains while higher cooling rates produce smaller grains and glass formation.

To study the competition between crystallization and vitrification, Mandadapu and co-workers proposed a simple but physically rich coarse-grained lattice model, called the Arrow-Potts model[21] that entails the essential physics of both glass-forming liquids and polycrystals. Specifically, the model supports a phase-transition between a liquid phase with glassy dynamics and a crystal phase with multiple orientations. As the name suggests, the Arrow-Potts model combines the Arrow model, which is a kinetically constrained model used in prior studies of glassy dynamics[49, 68], and the Potts model[69], a generalization of the Ising model. Using Monte Carlo simulations, the model reproduces the non-monotonic behaviors in time scales of crystallization as a function of temperature typically encoded in the time-temperature transformation (TTT) diagrams[70]. The model shows emergence of two classes of polycrystalline structures limited by crystal nucleation or growth. At high temperatures, crystallization is dominated by the nucleation of compact and fluctuating crystalline clusters. However, at low temperatures, crystal growth or coarsening proceeds through hierarchical relaxation pathways within the supercooled liquid, resulting in fractal and ramified crystals that contain large amount of interfaces.

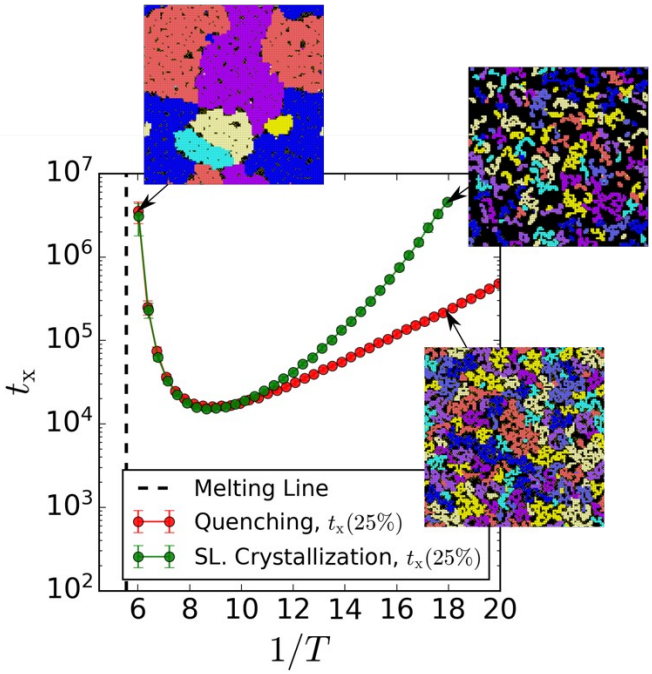

Figure 4: *TTT diagram showing crystallization times for a chosen crystal fraction of 25% as a function of temperature for two idealized protocols.* (i) Quenching a liquid state from above the melting temperature to a particular temperature *T* (red circles) and (ii) Crystallization of an equilibrated supercooled liquid (SL) at a particular temperature (Green circles). The dashed vertical line indicates the melting temperature. The TTT diagram from the model exhibits non-monotonic behaviors typical of many experimental TTD diagrams

on different materials. Furthermore, the two protocols show significant deviations in crystallization timescales when growing crystals at lower temperatures. Also shown are the microstructures with compact crystalline structures at high temperatures and fractal structures at low temperatures. Adapted from Ref. [21].

To explain and unify these two regimes, Mandadapu et. al. employed the framework of Kolmogorov-Johnson-Mehl-Avrami theory to combine the field theory of nucleation, and a random walk theory for crystal coarsening kinetics, both of which govern the high-T and low-T regimes respectively. Fig. 4 shows the non-monotonic behaviors of the crystallization time scales as a function of temperature when quenched or cooled from its liquid state to the crystalline state, along with the characteristic polycrystalline microstructures at high and low temperatures. As previously mentioned, grain boundary interfaces result from the mismatch of orientation of two single crystal grains that meet during a cooling protocol. The grain boundaries contribute an unfavorable energy to the system, and there is a strong thermodynamic driving force to eliminate them. Furthermore, the evolution of the microstructure in crystalline systems towards its equilibrium structure proceeds through the slow migration of grain boundaries. The structural and dynamical aspects of the grain boundaries in this process are therefore important to understanding how polycrystalline materials evolve over time. It is well known that boundaries through the small angle mismatched grains are known to consist of stacked dislocations with some order.[71-72]

However, the physical state and the dynamics of the high-angle grain boundaries are not completely understood. It is possible that just as the bulk liquid exists in liquid crystal and supercooled states, the grain boundaries may have a life of their own and exist in different states such as liquid, crystalline-like and disordered glassy states. These aspects provide interesting avenues for future studies of complex systems such as polycrystalline ice nucleation and growth, which has multiple crystalline polymorphs, in both bulk and under confinement.

4. CHEMICAL REACTIVITY AT INTERFACES

Chemical transformations in realistic systems rarely occur in a single phase and often involve transport and reactions across interfaces. Ahmed, Head-Gordon, Limmer and Wilson have examined the chemical coupling of bulk and interfacial processes to examine how reaction

mechanisms and rates are modified in systems that have simple interfaces and dimensions that are small compared to the characteristic reaction diffusion lengths.

The Diels-Alder (DA) and retro-DA reaction in bulk water is well understood and of great importance in organic chemistry. The Head-Gordon group recently studied the retro-Diels-Alder (retro-DA) reaction between cyclopentadiene (CPD) and methyl-vinyl-ketone (MVK) in bulk water at both low and high density, as well under two different manifestations of nanoconfinement (Fig. 5).[29] They simulated the entire system at the same level of QM theory, including the water molecules, with ab initio molecular dynamics (AIMD) based on density functional theory (DFT) using one of the best semi-local functional available, B97M-rV[73], which they have shown previously reproduces structural and dynamical properties of water at a level of accuracy on par with hybrid functionals[74]. To characterize the CPD-MVK retro-DA reaction in the different solvent environments, they mapped the free energy surface (FES) along two collective variables in the gas phase, bulk water at two different densities, and in two different nanoconfined environments, using well-tempered metadynamics.

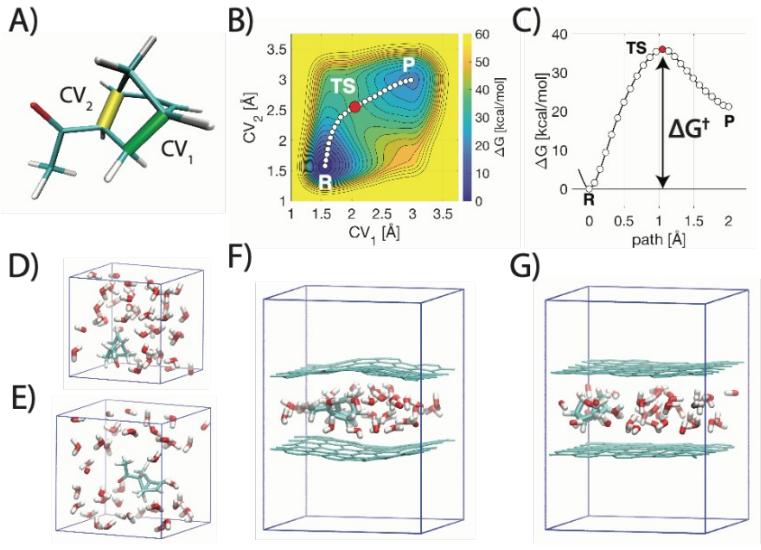

Figure 5. *The retro-Diels Alder in bulk vs. near confined interfaces*. (A) Collective variables CV_1 (green) and CV_2 (yellow) are the reactive bonds between diene and dienophile. (B,C) Free energy landscape, ΔG, from AIMD using B97M-rV projected in the CV space; the minimum energy path between the cycloadduct reactant and dissociated diene-dienophile products. (D-G) The different simulated solvent environments: bulk mass density ρ=1g/cm^3 and ρ=0.66g/cm^3 (D,E) and in water nanoconfined between bent (F) and flat (G) graphene sheets. Reprinted with permission from [29], copyright (2020) American Chemical Society

They found that low densities or nanoconfinement does not change the retro-DA activation free energies, and are comparable to those observed in bulk water within k_bT. These results are remarkable in that extremely different solvation environments lead to nearly identical acceleration rates. This is because the mechanism, which is the stabilization of the transition state

through a highly local water hydrogen bonding to promote the elongation of the first bond-breaking event, remains the same for all environments, including that under strong nanoconfinement. For this reason, the implications for on-water and microdroplet chemistry for accelerated Diels Alder reactions must be a complete mechanistic change, and possibly altering reactants so completely as to destroy the original reaction altogether.

This general conclusion from the Head-Gordon group that confinement effects on reactivity can be small for Diels-Alder reactions also resonates with the recent work of the Wilson group, who independently explored recent reports of dramatic reaction acceleration (up to 10^6 times) in electrospray droplets.[30] There is emerging evidence that chemical reactions in droplets, films and emulsions are accelerated by many orders of magnitude over the same reactions measured in macroscopic "beakers."[12, 28, 75-79] The molecular origin of these enhanced rates is not always known and in some cases may originate from the multiphase processes that occur in the electrospray droplets themselves.[30] These include solvent evaporation, which enhances bulk reaction rates as well as the possibility that interfering gas phase reactions; both of which confound observing in-droplet chemistry. Nevertheless, the droplet or aerosol interfaces play a substantial role in chemical transformations due to the much larger fraction of interfacial molecules with reduced solvent coordination (vs. bulk), and/or the charge state and surface acidity in micron-sized compartments.[76]

The reaction-diffusive length $\ell_{rxn} = \sqrt{D \cdot \tau}$ is the average distance a molecule travels prior to reaction. ℓ_{rxn} depends upon the diffusion constant (D) and τ, the chemical lifetime (i.e. concentration or bimolecular rate constant). For highly reactive species, such as hydroxyl radicals in an organic liquid, ℓ_{rxn} is only a couple of nanometers.[80] Less reactive molecules can also exhibit short ℓ_{rxn} in semisolid or glassy environments due to diffusive confinement.[81] It is our hypothesis that for reaction containers that have substantial surface area and dimensions that

are on the order of L_{rxn}, reactants increasingly sample the container walls (i.e. interfaces), where surface orientation and reduced solvent coordination can substantially alter transition states, rates, and mechanisms from those observed in the bulk liquid.

Figure 6. *Measurements for the heterogeneous reaction of OH with citric acid nanoparticles*. Reaction depth (L) vs. citric acid diffusion coefficient. Inset graphic showing L relative to the nanoparticle size.

For example, Wilson and coworkers studied the heterogeneous reaction of hydroxyl radicals (OH) with aqueous citric acid nanodroplets.[82-83] The diffusion constant of citric acid in aqueous solutions can be changed over many orders of magnitude by changing the relative humidity (R_H) around the droplet. This allows insight into how diffusive confinement (i.e. L_{rxn}) at the surfaces of glasses and semisolids (vs. liquids) alter the fundamental coupling of acid-base and free radical reaction pathways (Fig. 6). They found using surface sensitive mass spectrometry,[84-85] that the reaction depth was a sensitive function of the diffusion constant of citric acid in ~100 nm sized particles. At small diffusion coefficients, that reaction proceeded within 4-6 nm of a gas-particle surface, in contrast to larger diffusion coefficients where the entire particle contents were available for reaction. By simply changing the water content in the particle (by changing relative humidity) they were able to precisely change where the reaction occurs to explore more general aspects of how reaction pathways and intermediates depend upon nanoscale diffusively confined environments.

For aerosol particles that exist in highly viscous, diffusion-limited states, steep chemical gradients are expected to form during photochemical aging in the atmosphere. Under these conditions species at the aerosol surface are confined and become more rapidly transformed than molecules that are shielded and reside in the particle interior. To examine the formation and evolution of chemical gradients at aerosol interfaces, Wilson and Ahmed considered the heterogeneous reaction of hydroxyl radicals (OH) on ~200-nm particles of pure squalane (a

branched, liquid hydrocarbon) and octacosane (a linear, solid hydrocarbon), and binary mixtures of the two to understand how diffusion limitations and phase separation impact particle reactivity.[86] Aerosol mass spectrometry is used to measure the effective heterogeneous OH uptake coefficient and oxidation kinetics in the bulk, which are compared with the elemental composition of the surface obtained using X-ray photoemission. The differences in surface oxidation rates are analyzed using a previously published reaction diffusion model, which suggests that a 1-2 nm highly oxidized crust forms on octacosane particles, whereas in pure squalane the reaction products are homogenously mixed within the aerosol. This work illustrates how diffusion limitations can form particles with highly oxidized surfaces even at relatively low oxidant exposures, which is in turn expected to influence their microphysics in the atmosphere.

The Wilson group have also explored recent reports on dramatic acceleration (up to 10^6 times) in droplets. For the reported[87] phosphorylation reaction of sugars and the formation of ribonucleosides in droplets, careful control experiments have revealed in all likelihood that the observed reaction products and acceleration factors assigned to in-droplet chemistry have significant contributions from gas phase reactions.[88] Using a newly develop quadrupole electrodynamic trap they have further investigated confinement effects on a synthesis reaction using a fluorescent product. This approach allows precise control over droplet size (10 – 80 microns in diameter) and avoids some of the ambiguities of electrospray mass spectrometry. The rate coefficient for the reaction of *o*-phthalaldehyde (OPA) with alanine in the presence of dithiolthreitol was found[89] to be 25% larger than the equivalent reaction in the bulk, suggesting moderate effects of confinement on the bimolecular reaction.

Using stochastic reaction-diffusion simulations,[90] Wilson and co-workers have also examined accelerated imine synthesis in micro-emulsions reported by Fallah-Arraghi et al.[75] Imine formation from the reaction of an aldehyde and an amine is unfavorable in aqueous solutions. Yet Fallah-Arraghi et al., observed that imine synthesis was enhanced in micron-sized oil/water emulsions, with a 29-fold increase in the apparent equilibrium coefficient (K_{eq}^{obs}¿ favoring products. The Wilson lab were able to quantitatively simulate this increase in the equilibrium coefficient with emulsion radius (r) using a physically realistic surface thickness (δ) and rate coefficients for reaction, adsorption and desorption to the interface. These simulations showed the importance of equilibria (K_{eq}^{S}¿ at the surface and allowed a general kinetic

expression (Eq. 1) to be derived[90] to explain how reaction rates can be modified in micro-compartments.

$$K_{eq}^{obs} = K_{eq}^{S} \cdot f_s^{Amine} \cdot f_s^{Aldehyde} \cdot \left(\frac{r^3}{\left[r^3 - (r-\delta)^3 \right]} \right) + K_{eq}^{B} \quad (1)$$

A key feature illustrated in Eq. (1) is that it is the fraction of molecules (f_s¿ at the interface that plays a large role in governing reactivity in microdroplets.[90] For macroscale systems $f_s$is small so $K_{eq}^{obs} \approx K_{eq}^{B}$. However in micron-sized droplets or compartments f_s becomes sizable and in some cases (i.e. small compartments and dilute concentrations of reactions) can dominate the chemistry. This is illustrated in Fig. 7 where deviations from K_{eq}^{B} for imine synthesis become most pronounced in small compartments under dilute reactant concentrations (i.e. [aldehyde] and [amine]). For example, K_{eq}^{obs} is predicted to be nearly 5000x larger in a dilute, r = 8.4 μm emulsion, compared than a macroscale reaction vessel.

Figure 7. *Stochastic reaction-diffusion simulations for accelerated imine synthesis in micro-emulsions.* Predictions from Eq. (1) showing the scaling of the imine synthesis equilibrium constant (K_{eq}^{obs}¿ with size and aldehyde/amine concentrations. Adapted from [90] Published by The Royal Society of Chemistry.

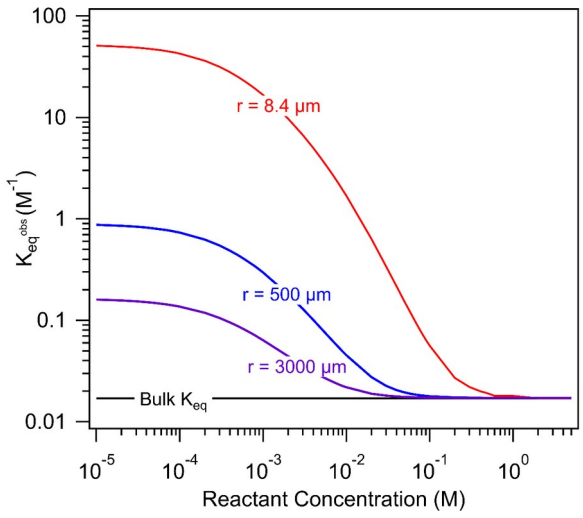

The Limmer group has married path sampling tools with advanced force-field representations to describe simple chemistries in

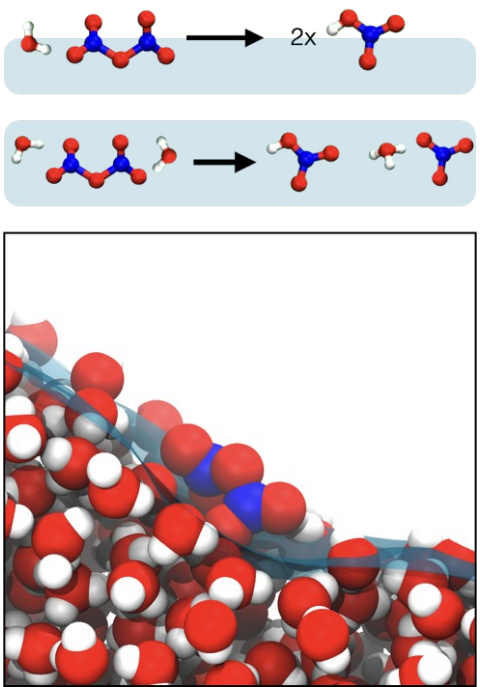

complex environments relevant to electrochemistry and atmospheric chemistry. Leveraging the isomorphism between rate constants and path ensemble partition functions, an algorithm to efficiently evaluate the spatial dependence of a rate constant, TPS+U, has been developed.[91] Standard umbrella sampling is added on top of transition path sampling to bias the likelihood of a reactive event occurring at particular locations in an inhomogeneous system, such as near to or away from an extended interface. This algorithm has been used to trace out the dramatic slowing down of ion pair dissociation in the proximity of a platinum electrode. This algorithmic advances clarified that the nearly two orders of magnitude decrease in the rate was due to slow solvation fluctuations of constrained water molecules strong confined to the first adlayer of the electrode.[92-93] The dependence of the rate of ion pair dissociation through the premelting layer of ice has also been evaluated.[94] As with the electrode interface, highly order water molecules at the liquid-solid interface were found to slow down dissociation, with a significant contribution to the rate afforded from the reduction of the effective diffusion controlling the reactive flux.

Figure 8. *N_2O_5 hydrolysis is dominated by interfacial reactions.* (top) at the liquid-vapor interface hydrolysis is proceeds to two in tact nitric acids while (middle) in the bulk the products are dissociated. (bottom) Characteristic configuration of N_2O_5 at the liquid-vapor interface with an intrinsic interface shown in cyan.

Galib and Limmer have studied the heterogeneous hydrolysis of N_2O_5, the primary sink of NOx compounds in the atmosphere, on the surface of aqueous aerosol (Fig. 8).[31] Such a study would be traditionally beyond the reach of standard computational tools due to the large time and length scales required to simulate interfacial chemical reactions with a realistic description of the environment. However, employing an artificial neural network based forcefield trained with ab initio reference data and employing importance sampling methods they were able to study the steps whereby a gaseous N_2O_5 molecule is reactively taken up in an aqueous aerosol. Contrary to traditional wisdom, and the prevailing assumptions of a generation of atmospheric chemists, they found this process was dominated by interfacial rather than bulk hydrolysis due to the fast kinetics and slow solvation. Beyond describing the thermodynamics and molecular dynamics that lead to reactive uptake, they proposed and validated a simple model of the reactive uptake that can serve as a foundation for future field studies and rationalize a broad range of existing observations.

5. WHERE THEORY AND EXPERIMENT MEET AT CATALYTIC INTERFACES

Synchrotron-based soft x-ray spectroscopies, namely soft x-ray absorption (XAS) and emission (XES) spectroscopy, resonant inelastic soft x-ray scattering (RIXS) and ambient pressure X-ray photoelectron spectroscopy (APXPS) with soft (<2 keV) and tender X-rays (2 keV to 6 keV) is necessary for characterizing interfacial chemistry between two condensed phases. Blum and Crumlin have intensively used these tools for the investigation of applied materials including thin-film solar cells[95], energy storage devices[96], and electrocatalytic devices[33, 42-46]. Due to the photon-in-photon-out nature of these soft X-ray experiments, it is possible to investigate both surface/gas and surface/liquid interfaces, making *in situ* and *operando* studies possible to answer the pertinent materials questions necessary for a further optimization of the various energy-related devices.

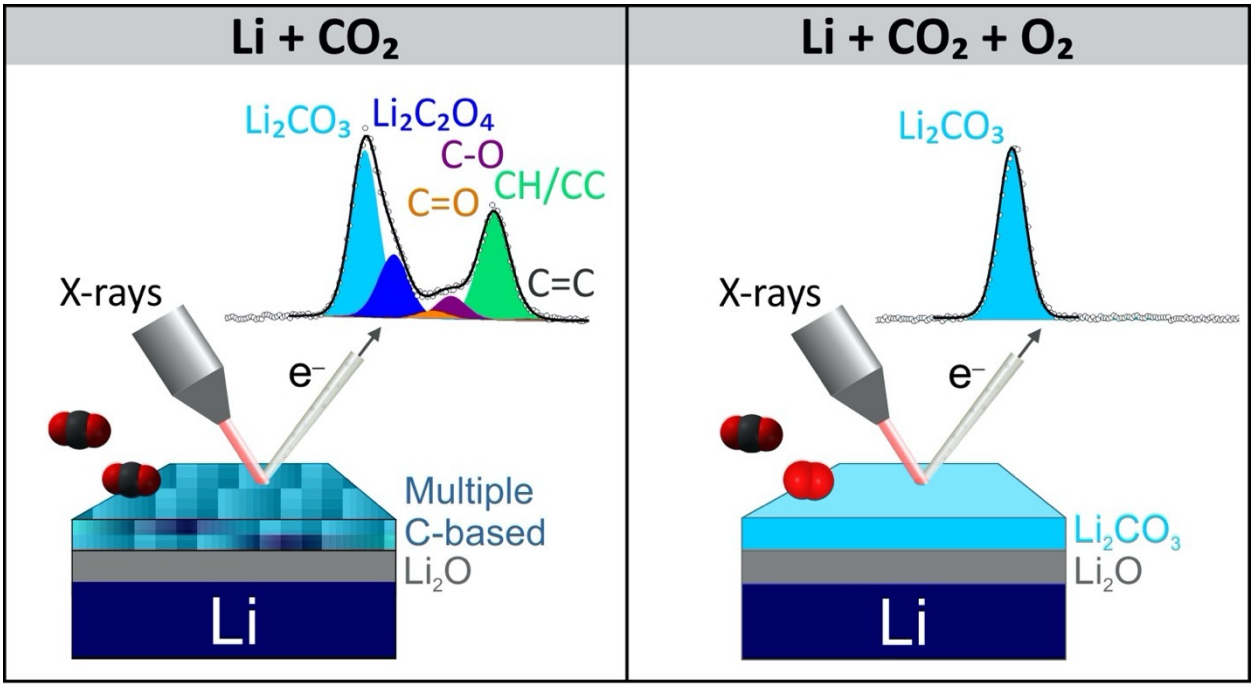

Figure 9. *APXPS studies of the interaction of lithium metal with CO_2* (a) gas as a function of time helped clarify the reaction pathway and main intermediates involved. (b) When O_2 gas is added to the environment, the reaction pathway is bypassed to directly promote carbonate as a single product. Reprinted with permission from [32], copyright (2020) American Chemical Society

Recently, Blum and Crumlin collaborated on APXPS work addressing the interaction of clean Li metal with CO_2 gas as a function of time and gas pressure (Fig. 9).[32] The experiments reveal that carbonate, oxalate, C-H/C-C, and LiO_2 evolve at the surface, whereas LiO_2 lies between Li^0 and the outermost carbonaceous component. Due to the peak evolution over time

and increasing pressure, the study clarifies the reaction pathway in which oxalate will be formed and react as reaction intermediate to create carbonate and CO. With the continued CO evolution, this pathway is self-recycling and can be proven by adding O_2 to the CO_2 gas environment. By adding O_2 to the gas composition, the surface is completely oxidized, and no oxalate intermediate formation is evolving. Thus, the reaction pathway is bypassed and carbonate is dominating the sample surface.

The Crumlin lab have shown that the utilization of APXPS revealed how CO_2 interacts with a copper vs silver metal surface and how the water changed the adsorbates surface bonding properties.[45-46] On the Cu(111) surface the initial physisorption of linear CO_2 and its transformation to a chemisorbed bent CO_2 when water was introduced is a transition that occurs on the time scale of minutes to reach equilibrium. When both water and CO_2 are subsequently removed, they observed the stable bent CO_2 remaining on the surface confirming its strong bond to the surface. However, one of the challenges for characterizing metastable states, intermediates, and chemical reactions previously unobserved, is the identification of what is measured using APXPS and other surface sensitive techniques. To address this challenge, a Density Functional Theory (DFT) prediction approach that simulates absorbate configurations and their respective free energies help interpret experimental observables such as the measured binding energies. This process is depicted in Fig. 10 that shows how CO_2 interacting this time with a silver surface and its transformation when exposed to water both through QM predictions and their agreement with experimentally collected APXPS data.

However DFT at the lower rungs of Jacob's ladder has yielded mixed success for modeling metal surfaces important to heterogeneous catalysis.[97-100] Just recently a benchmark study[101] for metal surface relaxations and adsorption energies and site preferences for CO on the M(111) where M = Pt, Cu, Ag, Au metal surfaces found that while RPBE performed, more recent meta-GGA DFT functionals such as SCAN[102-103] and B97M-rV[73, 104] exhibited under-relaxed surfaces and

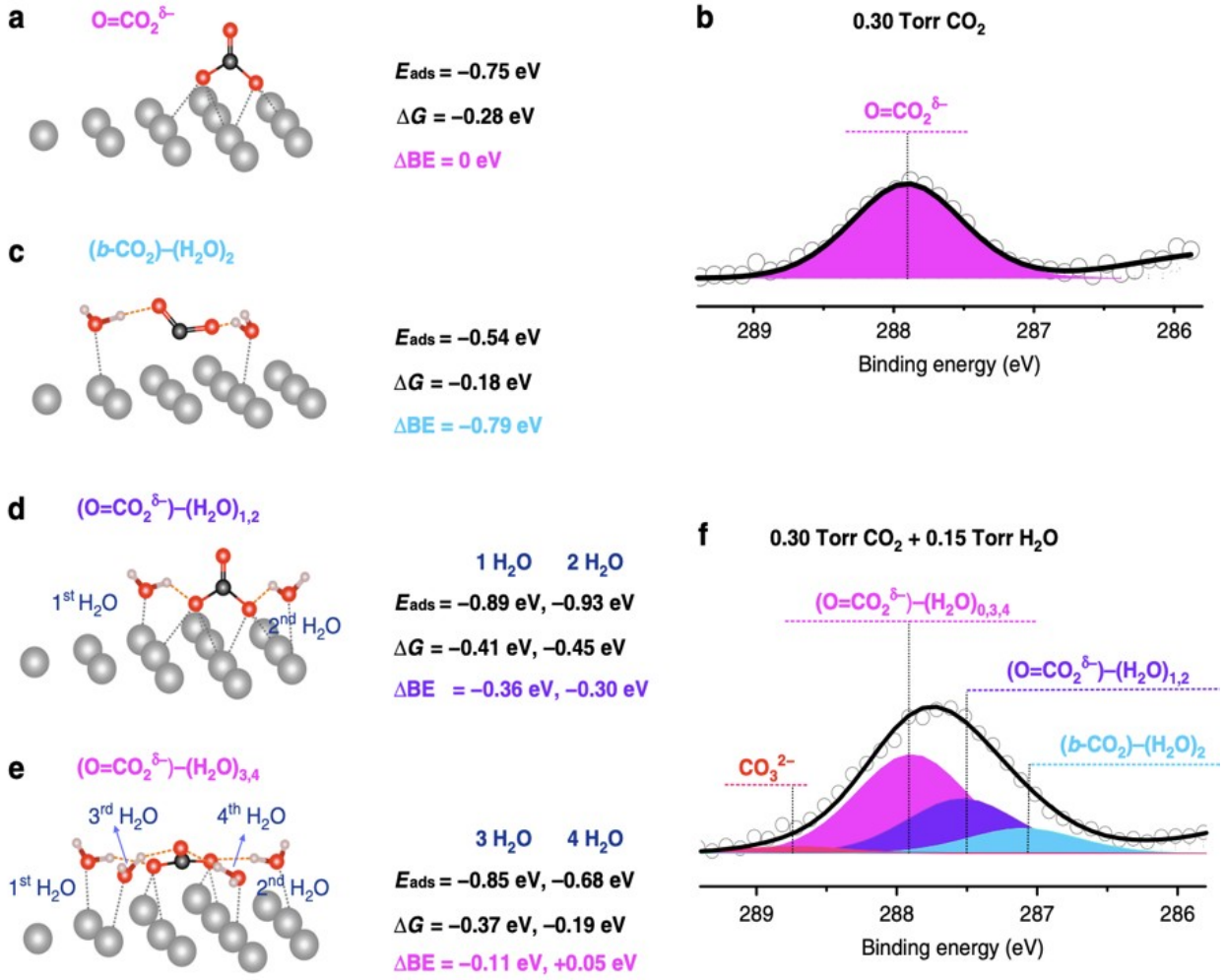

Figure 10. *QM predictions and experimental observations of Ag surface with CO_2 adsorption alone and with H_2O at 298 K*. **a)** Predicted structures for O = $CO_2^{\delta-}$ on Ag surface. **b)** C 1s APXPS spectra for Ag surfaces in presence of 0.3 Torr CO_2 at 298 K. **c)** b-CO_2 becomes stabilized by a pair of H_2Oad forming HB's with ΔG of −0.18 eV with respect to desorbing H_2O and CO_2. **d, e)** Adsorbed O = $CO_2^{\delta-}$ stabilizes one or two H_2Oad via HBs and two more water with HBs to the Oup. O = $CO_2^{\delta-}$ stabilizes the 1st, 2nd, 3rd, and 4th H_2O on this site with ΔG of −0.41 eV, −0.45 eV, −0.37 eV, and −0.19 eV, respectively. **f)** C 1s APXPS spectra and the theoretical peak deconvolution results for Ag surfaces in the presence of 0.3 Torr CO_2 and 0.15 Torr H_2O at 298 K. Figure reproduced from [46].

strong overbinding of CO, and did not predict the *atop* site for all metals observed at low CO adsorbate coverage. But rarely are DFT functionals evaluated at the finite temperature conditions that are manifest in all catalytic experiments.[105-106] To address this important aspect of electrocatalysis modeling, the Head-Gordon lab used AIMD in the NVT and NPT ensembles to better and more directly simulate the natural statistical fluctuations of an electrocatalytic surface under ambient conditions.[35] They found that the good agreement for RPBE at 0K worsened with

experiment at finite temperature, whereas the B97M–rV[73, 104] meta-GGA functional better reproduced experimental bulk and surface relaxation properties. In turn the CO adsorption energies and site preferences on the M(111) surfaces (where M = Pt, Cu, Ag, Au) using the meta-GGA functional also improved, predicting the *atop* site preference and correct trend for the remaining multi-coordinated sites. Thermalization exposes the importance of dispersion interactions, for which the B97M-rV functional accurately predicts the weak binding energetics for the Ag(111) and Au(111) metals, and were found to be a mixture of chemisorbed and physisorbed CO species. Finally because the B97M–rV[73, 104] functional also provides an excellent description of bulk water[74, 107], it reveals its potential feasibility for better theoretical predictions at the solid-liquid interface in the future.

6. DISCUSSION AND FUTURE DIRECTIONS

Some future directions for interfacial chemistry is to increase the level of integration of spectroscopic tools with scattering methods to be able to decipher the complex behavior on interfaces in order to deepen connections to theory. The IR and THz region of the water spectrum is highly affected by its hydrogen-bonding environment[108] and is thus an excellent probe for the effect of electric field on its properties[109] and will be applied to problems of ice nucleation under confinement and for electric fields on chemical reactivity as shown by the Head-Gordon lab[34, 36]. Attenuated Total Reflection (ATR), which allows direct insight into the aqueous interface and the double layer on electrocatalytic surfaces, could also be readily applied[110] and coupled into the experimental platform. The beamlines at the Advanced Light Source (ALS), which is over 25 years old, will benefit from a new initiative to upgrade the ALS to a diffraction-limited storage ring (DLSR)[111] that has full transverse coherence in its light output. The new capabilities will allow us to bridge the fundamental electronic, structural, and chemical dynamics of collective phenomena of extended systems in the condensed phase.[112] Emerging exceptionally powerful X-ray spectroscopy methods such as APXPS[113] and RIXS[114] with sub-natural line width, as demonstrated recently to elucidate structure of water,[115] heroic work for 3rd generation light sources, will be routine at DLSRs. The studies anticipated by Blum on the use of flat and merged jets and Ahmed to couple X-Ray scattering to spectroscopy[116] to probe dynamics will also benefit enormously from this new capability.

Development of a synergistic experimental and theory framework at the chemical beamlines at the ALS will enable the acceleration for future investigations to understand absorbate and solvent interactions on arbitrary metal surfaces and/or provide greater time- and space-resolution for understanding interfacial reactions. However, figuring out a seamless way of coupling theory and experiment to elucidate mechanisms poses a major challenge. Crumlin and co-workers have proposed creating a "Digital Twin",[117] the direct computational simulation of a device or system, which would eventually augment decision making and execution of optimal experimental strategies to drive physical knowledge acquisition for reactive systems of interests. This poses a huge challenge to a theoretical framework that is robust enough to match experimental capabilities, that it is efficient enough to "reply" to continuous updates from real experiments, and that predictive capabilities are strong enough to effect correct experimental adjustments. We envision that electronic structure calculations, statistical mechanical sampling to capture grand canonical statistics and reaction path finding, can be coupled with workflows that can create massively parallel physical simulations that leverage leadership class computational resources. One could imagine that the simulation data will be further elaborated with data analytics or simulated with deep learning[118] in order to construct massive chemical reaction networks[119] et al that will yield fundamental mechanistic understanding about catalytic and electrochemical reaction cascades to connect to *experiments on* a range of materials, solutions, and across experimental conditions.

Many of the efforts discussed above occur near enough to equilibrium that standard concepts like free energies and transition states can be used to rationalize observations. An exciting future direction concerns the development of formalisms, numerical and experimental tools to probe molecular properties and chemical transformations in instances far from equilibrium. When reactions are driven through photoexcitation and large energies must be dissipated in complex environments, nonequilibrium and nonadiabatic effects must be described on the same footing. Advances in the molecular theory of open quantum systems can provide guidance[120-122] for what quantities encode molecular dynamics most transparently. Further, far from equilibrium conditions occur ubiquitously in confined systems where driving forces and relaxation times can be large. Advances in driven confined liquids would benefit disparate fields like separations, energy storage and generation, and atmospheric chemistry. Generalizations of

transition state theory valid away from equilibrium,[48] and notions of variational stability[123-124] recently developed can aid in guiding experimental design.

CONFLICT OF INTEREST. The authors declare no conflict of interest

ACKNOWLEDGEMENTS. We give our collective best to Daniel Neumark in his 65th year and wish him many more years of fruitful research in his evolving direction toward the condensed phase. This research was supported under the CPIMS program by the Director, Office of Science, Office of Basic Energy Sciences, Chemical Sciences Division of the U.S. Department of Energy under Contract No. DE-AC02-05CH11231. This research used resources of the Advanced Light Source, which is a DOE Office of Science User Facility under Contract No. DE-AC02-05CH11231. This research used resources of the National Energy Research Scientific Computing Center, a DOE Office of Science User Facility supported by the Office of Science of the U.S. Department of Energy under Contract No. DE-AC02-05CH11231.

REFERENCES

1. Rubasinghege, G.; Grassian, V. H. Role(s) of adsorbed water in the surface chemistry of environmental interfaces. *Chem. Comm.* **2013,** *49* (30), 3071-3094.
2. Tirrell, M.; Hubbard, S.; Sholl, D. *Basic Research Needs for Energy and Water*; Washington DC, 2018; pp 1-102.
3. Strong, S. E.; Eaves, J. D. Atomistic Hydrodynamics and the Dynamical Hydrophobic Effect in Porous Graphene. *J. Phys. Chem. Lett.* **2016,** *7* (10), 1907-1912.
4. Geise Geoffrey, M.; Lee, H. S.; Miller Daniel, J.; Freeman Benny, D.; McGrath James, E.; Paul Donald, R. Water purification by membranes: The role of polymer science. *J. Poly. Sci. B: Poly. Phys.s* **2010,** *48* (15), 1685-1718.
5. Bocquet, L. Nanofluidics coming of age. *Nature Materials* **2020,** *19* (3), 254-256.
6. Stupp, S. I.; Zha, R. H.; Palmer, L. C.; Cui, H.; Bitton, R. Self-assembly of biomolecular soft matter. *Faraday Discuss* **2013,** *166*, 9-30.
7. *Basic Research Needs for Catalysis Science to Transform Energy Technologies*; 2017.
8. Barr, C. M.; Thomas, S.; Hart, J. L.; Harlow, W.; Anber, E.; Taheri, M. L. Tracking the evolution of intergranular corrosion through twin-related domains in grain boundary networks. *npj Materials Degradation* **2018,** *2* (1), 14.
9. Finlayson-Pitts, B. J.; Wingen, L. M.; Perraud, V.; Ezell, M. J. Open questions on the chemical composition of airborne particles. *Comm. Chem.* **2020,** *3* (1), 108.
10. Donaldson, D. J.; Vaida, V. The Influence of Organic Films at the Air−Aqueous Boundary on Atmospheric Processes. *Chem. Rev.* **2006,** *106* (4), 1445-1461.
11. Zhong, J.; Zhu, C.; Li, L.; Richmond, G. L.; Francisco, J. S.; Zeng, X. C. Interaction of SO2 with the Surface of a Water Nanodroplet. *J. Am. Chem. Soc.* **2017,** *139* (47), 17168-17174.

12. Wei, Z.; Li, Y.; Cooks, R. G.; Yan, X. Accelerated Reaction Kinetics in Microdroplets: Overview and Recent Developments. *Ann. Rev. Phys. Chem.* **2020,** *71* (1), 31-51.
13. Griffith, E. C.; Vaida, V. In situ observation of peptide bond formation at the water–air interface. *Proc. Natl. Acad. Sci.* **2012,** *109* (39), 15697.
14. Anglada, J. M.; Martins-Costa, M. T. C.; Francisco, J. S.; Ruiz-López, M. F. Reactivity of Undissociated Molecular Nitric Acid at the Air–Water Interface. *J. Am. Chem. Soc.* **2021,** *143* (1), 453-462.
15. Shultz, M. J. Crystal growth in ice and snow. *Physics Today* **2018,** *71* (2), 34-39.
16. Björneholm, O.; Hansen, M. H.; Hodgson, A.; Liu, L.-M.; Limmer, D. T.; Michaelides, A.; Pedevilla, P.; Rossmeisl, J.; Shen, H.; Tocci, G.; Tyrode, E.; Walz, M.-M.; Werner, J.; Bluhm, H. Water at Interfaces. *Chem. Rev.* **2016,** *116* (13), 7698-7726.
17. Otten, D. E.; Shaffer, P. R.; Geissler, P. L.; Saykally, R. J. Elucidating the mechanism of selective ion adsorption to the liquid water surface. *Proc. Natl. Acad. Sci.* **2012,** *109* (3), 701.
18. McCaffrey, D. L.; Nguyen, S. C.; Cox, S. J.; Weller, H.; Alivisatos, A. P.; Geissler, P. L.; Saykally, R. J. Mechanism of ion adsorption to aqueous interfaces: Graphene/water vs. air/water. *Proc. Natl. Acad. Sci.* **2017,** *114* (51), 13369.
19. Huang, Z.; Kaur, S.; Ahmed, M.; Prasher, R. Water Freezes at Near-Zero Temperatures Using Carbon Nanotube-Based Electrodes under Static Electric Fields. *ACS Appl Mater Interfaces* **2020,** *12* (40), 45525-45532.
20. Pestana, L. R.; Felberg, L. E.; Head-Gordon, T. Coexistence of Multilayered Phases of Confined Water: The Importance of Flexible Confining Surfaces. *ACS Nano* **2018,** *12* (1), 448-454.
21. Hasyim, M. R.; Mandadapu, K. K. Theory of crystallization versus vitrification. *arXiv:2103.12389* **2020**.
22. Wolff, E. W.; Mulvaney, R.; Oates, K. Diffusion and location of hydrochloric acid in ice: Implications for polar stratospheric clouds and ozone depletion. *Geophys. Res. Lett.* **1989,** *16* (6), 487-490.
23. Wolff, E. W. In *Location, Movement and Reactions of Impurities in Solid Ice*, Chemical Exchange Between the Atmosphere and Polar Snow, Berlin, Heidelberg, 1996; Wolff, E. W.; Bales, R. C., Eds. Springer Berlin Heidelberg: Berlin, Heidelberg, 1996; pp 541-560.
24. Abbatt, J. P. D. Interactions of Atmospheric Trace Gases with Ice Surfaces: Adsorption and Reaction. *Chem. Rev.* **2003,** *103* (12), 4783-4800.
25. Huthwelker, T.; Ammann, M.; Peter, T. The Uptake of Acidic Gases on Ice. *Chem. Rev.* **2006,** *106* (4), 1375-1444.
26. Huthwelker, T.; Lamb, D.; Baker, M.; Swanson, B.; Peter, T. Uptake of SO2 by Polycrystalline Water Ice. *J. Coll. Inter. Sci.* **2001,** *238* (1), 147-159.
27. Narayan, S.; Muldoon, J.; Finn, M. G.; Fokin, V. V.; Kolb, H. C.; Sharpless, K. B. "On Water": Unique Reactivity of Organic Compounds in Aqueous Suspension. *Angew. Chem. Int. Ed.* **2005,** *44* (21), 3275-3279.
28. Lee, J. K.; Banerjee, S.; Nam, H. G.; Zare, R. N. Acceleration of reaction in charged microdroplets. *Quart. Rev. Biophys.* **2015,** *48* (4), 437-444.
29. Pestana, L. R.; Hao, H.; Head-Gordon, T. Diels-Alder Reactions in Water Are Determined by Microsolvation. *Nano Lett* **2020,** *20* (1), 606-611.

30. Rovelli, G.; Jacobs, M. I.; Willis, M. D.; Rapf, R. J.; Prophet, A. M.; Wilson, K. R. A critical analysis of electrospray techniques for the determination of accelerated rates and mechanisms of chemical reactions in droplets. *Chem. Sci.* **2020,** *11* (48), 13026-13043.
31. Galib, M.; Limmer, D. T. Reactive uptake of N2O5 by atmospheric aerosol is dominated by interfacial processes. *Science* **2021,** *371* (6532), 921.
32. Etxebarria, A.; Yun, D.-J.; Blum, M.; Ye, Y.; Sun, M.; Lee, K.-J.; Su, H.; Muñoz-Márquez, M. Á.; Ross, P. N.; Crumlin, E. J. Revealing In Situ Li Metal Anode Surface Evolution upon Exposure to CO2 Using Ambient Pressure X-Ray Photoelectron Spectroscopy. *ACS Applied Materials & Interfaces* **2020,** *12* (23), 26607-26613.
33. Favaro, M.; Jeong, B.; Ross, P. N.; Yano, J.; Hussain, Z.; Liu, Z.; Crumlin, E. J. Unravelling the electrochemical double layer by direct probing of the solid/liquid interface. *Nature Comm.* **2016,** *7*.
34. Welborn, V. V.; Ruiz Pestana, L.; Head-Gordon, T. Computational optimization of electric fields for better catalysis design. *Nature Catalysis* **2018,** *1* (9), 649-655.
35. Li, W.-L.; Lininger, C. N.; Welborn, V. V.; Rossomme, E.; Bell, A. T.; Head-Gordon, M.; Head-Gordon, T. Statistical Mechanics Improves Density Functional Theory for Electrocatalytic Metal Surface Properties and CO Binding Trends. *(arXiv:2006.03971)* **2021**.
36. Li, W. L.; Head-Gordon, T. Catalytic Principles from Natural Enzymes and Translational Design Strategies for Synthetic Catalysts. *ACS Cent. Sci.* **2021,** *7* (1), 72-80.
37. Davis, R. D.; Jacobs, M. I.; Houle, F. A.; Wilson, K. R. Colliding-Droplet Microreactor: Rapid On-Demand Inertial Mixing and Metal-Catalyzed Aqueous Phase Oxidation Processes. *Anal. Chem.* **2017,** *89* (22), 12494-12501.
38. Smith, J. W.; Saykally, R. J. Soft X-ray Absorption Spectroscopy of Liquids and Solutions. *Chem. Rev.* **2017,** *117* (23), 13909-13934.
39. Kostko, O.; Xu, B.; Jacobs, M. I.; Ahmed, M. Soft X-ray spectroscopy of nanoparticles by velocity map imaging. *J. Chem. Phys.* **2017,** *147* (1), 013931.
40. Ahmed, M.; Kostko, O. From atoms to aerosols: probing clusters and nanoparticles with synchrotron based mass spectrometry and X-ray spectroscopy. *Phys. Chem. Chem. Phys.* **2020,** *22* (5), 2713-2737.
41. Weeraratna, C.; Amarasinghe, C.; Lu, W.; Ahmed, M. A Direct Probe of the Hydrogen Bond Network in Aqueous Glycerol Aerosols. *J. Phys. Chem. Lett.* **2021**, *12*, 5503-5511.
42. Axnanda, S.; Crumlin, E. J.; Mao, B. H.; Rani, S.; Chang, R.; Karlsson, P. G.; Edwards, M. O. M.; Lundqvist, M.; Moberg, R.; Ross, P.; Hussain, Z.; Liu, Z. Using "Tender" X-ray Ambient Pressure X-Ray Photoelectron Spectroscopy as A Direct Probe of Solid-Liquid Interface. *Scientific Reports* **2015,** *5(1),* 9788.
43. Crumlin, E. J.; Liu, Z.; Bluhm, H.; Yang, W. L.; Guo, J. H.; Hussain, Z. X-ray spectroscopy of energy materials under in situ/operando conditions. *J. Elect. Spect. Related Phenomena* **2015,** *200*, 264-273.
44. Favaro, M.; Valero-Vidal, C.; Eichhorn, J.; Toma, F. M.; Ross, P. N.; Yano, J.; Liu, Z.; Crumlin, E. J. Elucidating the alkaline oxygen evolution reaction mechanism on platinum. *J. Mat. Chem. A* **2017,** *5* (23), 11634-11643.
45. Favaro, M.; Xiao, H.; Cheng, T.; Goddard, W. A.; Yano, J.; Crumlin, E. J. Subsurface oxide plays a critical role in CO2 activation by Cu(111) surfaces to form chemisorbed CO2, the first step in reduction of CO2. *Proc. Natl. Acad. Sci. USA* **2017,** *114* (26), 6706-6711.

46. Ye, Y. F.; Yang, H.; Qian, J.; Su, H. Y.; Lee, K. J.; Cheng, T.; Xiao, H.; Yano, J.; Goddard, W. A.; Crumlin, E. J. Dramatic differences in carbon dioxide adsorption and initial steps of reduction between silver and copper. *Nature Comm.* **2019,** *10*, 1875.
47. Pestana, L. R.; Minnetian, N.; Lammers, L. N.; Head-Gordon, T. Dynamical inversion of the energy landscape promotes non-equilibrium self-assembly of binary mixtures. *Chem. Sci.* **2018,** *9* (6), 1640-1646.
48. Kuznets-Speck, B.; Limmer, D. T. Dissipation bounds the amplification of transition rates far from equilibrium. *Proc. Natl. Acad. Sci.* **2021,** *118* (8), e2020863118.
49. Katira, S.; Garrahan, J. P.; Mandadapu, K. K. Theory for Glassy Behavior of Supercooled Liquid Mixtures. *Phys. Rev. Lett.* **2019,** *123* (10), 100602.
50. Rotskoff, G. M.; Geissler, P. L. Robust nonequilibrium pathways to microcompartment assembly. *Proc. Natl. Acad. Sci.* **2018,** *115* (25), 6341.
51. Duignan, T. T.; Baer, M. D.; Schenter, G. K.; Mundy, C. J. Real single ion solvation free energies with quantum mechanical simulation. *Chem. Sci.* **2017,** *8* (9), 6131-6140.
52. Yeh, I.-C.; Hummer, G. System-Size Dependence of Diffusion Coefficients and Viscosities from Molecular Dynamics Simulations with Periodic Boundary Conditions. *J. Phys. Chem. B* **2004,** *108* (40), 15873-15879.
53. Jungwirth, P.; Tobias, D. J. Specific Ion Effects at the Air/Water Interface. *Chem. Rev.* **2006,** *106* (4), 1259-1281.
54. Mizuno, H.; Rizzuto, A. M.; Saykally, R. J. Charge-Transfer-to-Solvent Spectrum of Thiocyanate at the Air/Water Interface Measured by Broadband Deep Ultraviolet Electronic Sum Frequency Generation Spectroscopy. *J. Phys. Chem. Lett.* **2018,** *9* (16), 4753-4757.
55. Cox, S. J.; Geissler, P. L. Interfacial ion solvation: Obtaining the thermodynamic limit from molecular simulations. *J. Chem. Phys.* **2018,** *148* (22), 222823.
56. Cox, S. J.; Mandadapu, K. K.; Geissler, P. L. Quadrupole-mediated dielectric response and the charge-asymmetric solvation of ions in water. *arXiv:2103.12389* **2021**.
57. Koop, T.; Luo, B.; Tsias, A.; Peter, T. Water activity as the determinant for homogeneous ice nucleation in aqueous solutions. *Nature* **2000,** *406*, 611.
58. Lo, C.-W.; Sahoo, V.; Lu, M.-C. Control of Ice Formation. *ACS Nano* **2017,** *11* (3), 2665-2674.
59. He, Z.; Liu, K.; Wang, J. Bioinspired materials for controlling ice nucleation, growth, and recrystallization. *Acc. Chem. Res.* **2018,** *51* (5), 1082-1091.
60. Zhang, Z.; Liu, X.-Y. Control of ice nucleation: freezing and antifreeze strategies. *Chem. Soc. Rev.* **2018**, *47,* 7116-7139
61. Bigg, E. K. The supercooling of water. *Proc. Phys. Soc. Sect. B* **1953,** *66* (8), 688.
62. Sellberg, J. A.; Huang, C.; McQueen, T. A.; Loh, N. D.; Laksmono, H.; Schlesinger, D.; Sierra, R. G.; Nordlund, D.; Hampton, C. Y.; Starodub, D.; DePonte, D. P.; Beye, M.; Chen, C.; Martin, A. V.; Barty, A.; Wikfeldt, K. T.; Weiss, T. M.; Caronna, C.; Feldkamp, J.; Skinner, L. B.; Seibert, M. M.; Messerschmidt, M.; Williams, G. J.; Boutet, S.; Pettersson, L. G. M.; Bogan, M. J.; Nilsson, A. Ultrafast X-ray probing of water structure below the homogeneous ice nucleation temperature. *Nature* **2014,** *510*, 381.
63. Naullage, P. M.; Qiu, Y.; Molinero, V. What Controls the Limit of Supercooling and Superheating of Pinned Ice Surfaces? *J. Phys. Chem. Lett.* **2018,** *9* (7), 1712-1720.

64. Mossop, S. The freezing of supercooled water. *Proc. Phys. Soc.. Sect. B* **1955,** *68* (4), 193.
65. Moore, E. B.; Molinero, V. Structural transformation in supercooled water controls the crystallization rate of ice. *Nature* **2011,** *479*, 506.
66. Algara-Siller, G.; Lehtinen, O.; Wang, F. C.; Nair, R. R.; Kaiser, U.; Wu, H. A.; Geim, A. K.; Grigorieva, I. V. Square ice in graphene nanocapillaries. *Nature* **2015,** *519* (7544), 443-445.
67. Neek-Amal, M.; Peeters, F. M.; Grigorieva, I. V.; Geim, A. K. Commensurability Effects in Viscosity of Nanoconfined Water. *ACS Nano* **2016,** *10* (3), 3685-3692.
68. Garrahan, J. P.; Chandler, D. Coarse-grained microscopic model of glass formers. *Proc. Natl. Acad. Sci.* **2003,** *100* (17), 9710.
69. Wu, F. Y. The Potts model. *Rev. Mod. Phys.* **1982,** *54* (1), 235-268.
70. Masuhr, A.; Waniuk, T. A.; Busch, R.; Johnson, W. L. Time Scales for Viscous Flow, Atomic Transport, and Crystallization in the Liquid and Supercooled Liquid States of *Zr41.2Ti13.8Cu12.5Ni10.0Be22.5*. *Phys. Rev. Lett.* **1999,** *82* (11), 2290-2293.
71. Read, W. T.; Shockley, W. Dislocation Models of Crystal Grain Boundaries. *Phys. Rev.* **1950,** *78* (3), 275-289.
72. Sutton, A. P.; Balluffi, R. W. *Interfaces in Crystalline Materials*. Oxford University Press: Oxford, 1995.
73. Mardirossian, N.; Head-Gordon, M. Mapping the genome of meta-generalized gradient approximation density functionals: The search for B97M-V. *J. Chem. Phys.* **2015,** *142* (7), 074111.
74. Ruiz Pestana, L.; Marsalek, O.; Markland, T. E.; Head-Gordon, T. The Quest for Accurate Liquid Water Properties from First Principles. *J. Phys. Chem. Lett.* **2018,** *9* (17), 5009-5016.
75. Fallah-Araghi, A.; Meguellati, K.; Baret, J.-C.; Harrak, A. E.; Mangeat, T.; Karplus, M.; Ladame, S.; Marques, C. M.; Griffiths, A. D. Enhanced Chemical Synthesis at Soft Interfaces: A Universal Reaction-Adsorption Mechanism in Microcompartments. *Phys. Rev. Lett.* **2014,** *112* (2), 028301.
76. Yan, X.; Bain, R. M.; Cooks, R. G. Organic Reactions in Microdroplets: Reaction Acceleration Revealed by Mass Spectrometry. *Angew. Chem. Int. Ed.* **2016,** *55* (42), 12960-12972.
77. Banerjee, S.; Gnanamani, E.; Yan, X.; Zare, R. N. Can all bulk-phase reactions be accelerated in microdroplets? *Analyst* **2017,** *142* (9), 1399-1402.
78. Lee, J. K.; Walker, K. L.; Han, H. S.; Kang, J.; Prinz, F. B.; Waymouth, R. M.; Nam, H. G.; Zare, R. N. Spontaneous generation of hydrogen peroxide from aqueous microdroplets. *Proc. Natl. Acad. Sci.* **2019,** *116* (39), 19294.
79. Li, Y.; Mehari, T. F.; Wei, Z.; Liu, Y.; Cooks, R. G. Reaction Acceleration at Air-Solution Interfaces: Anisotropic Rate Constants for Katritzky Transamination. *J. Mass Spect.* **2021,** *56*, e4585.
80. Lee, L.; Wilson, K. The Reactive–Diffusive Length of OH and Ozone in Model Organic Aerosols. *J. Phys. Chem. A* **2016,** *120* (34), 6800-6812.

81. Wiegel, A. A.; Liu, M. J.; Hinsberg, W. D.; Wilson, K. R.; Houle, F. A. Diffusive confinement of free radical intermediates in the OH radical oxidation of semisolid aerosols. *Phys. Chem. Chem. Phys.* **2017,** *19* (9), 6814-6830.
82. Davies, J. F.; Wilson, K. R. Nanoscale interfacial gradients formed by the reactive uptake of OH radicals onto viscous aerosol surfaces. *Chem. Sci.* **2015,** *6* (12), 7020-7027.
83. Liu, M. J.; Wiegel, A. A.; Wilson, K. R.; Houle, F. A. Aerosol Fragmentation Driven by Coupling of Acid–Base and Free-Radical Chemistry in the Heterogeneous Oxidation of Aqueous Citric Acid by OH Radicals. *J. Phys. Chem. A* **2017,** *121* (31), 5856-5870.
84. Chan, M. N.; Nah, T.; Wilson, K. R. Real time in situ chemical characterization of sub-micron organic aerosols using Direct Analysis in Real Time mass spectrometry (DART-MS): the effect of aerosol size and volatility. *Analyst* **2013,** *138* (13), 3749-3757.
85. Nah, T.; Chan, M.; Leone, S. R.; Wilson, K. R. Real Time in Situ Chemical Characterization of Submicrometer Organic Particles Using Direct Analysis in Real Time-Mass Spectrometry. *Anal. Chem.* **2013,** *85* (4), 2087-2095.
86. Jacobs, M. I.; Xu, B.; Kostko, O.; Wiegel, A. A.; Houle, F. A.; Ahmed, M.; Wilson, K. R. Using Nanoparticle X-ray Spectroscopy to Probe the Formation of Reactive Chemical Gradients in Diffusion-Limited Aerosols. *J. Phys. Chem. A* **2019,** *123* (28), 6034-6044.
87. Nam, I.; Lee, J. K.; Nam, H. G.; Zare, R. N. Abiotic production of sugar phosphates and uridine ribonucleoside in aqueous microdroplets. *Proc. Natl. Acad. Sci.* **2017,** *114* (47), 12396.
88. Jacobs, M. I.; Davis, R. D.; Rapf, R. J.; Wilson, K. R. Studying Chemistry in Micro-compartments by Separating Droplet Generation from Ionization. *J. Am. Soc. Mass Spectr.* **2019,** *30* (2), 339-343.
89. Jacobs, M. I.; Davies, J. F.; Lee, L.; Davis, R. D.; Houle, F.; Wilson, K. R. Exploring Chemistry in Microcompartments Using Guided Droplet Collisions in a Branched Quadrupole Trap Coupled to a Single Droplet, Paper Spray Mass Spectrometer. *Anal. Chem.* **2017,** *89* (22), 12511-12519.
90. Wilson, K. R.; Prophet, A. M.; Rovelli, G.; Willis, M. D.; Rapf, R. J.; Jacobs, M. I. A kinetic description of how interfaces accelerate reactions in micro-compartments. *Chem. Sci.* **2020,** *11* (32), 8533-8545.
91. Schile, A. J.; Limmer, D. T. Rate constants in spatially inhomogeneous systems. *J. Chem. Phys.* **2019,** *150* (19), 191102.
92. Limmer, D. T.; Willard, A. P.; Madden, P.; Chandler, D. Hydration of metal surfaces can be dynamically heterogeneous and hydrophobic. *Proc. Natl. Acad. Sci.* **2013,** *110* (11), 4200.
93. Kattirtzi, J. A.; Limmer, D. T.; Willard, A. P. Microscopic dynamics of charge separation at the aqueous electrochemical interface. *Proc. Natl. Acad. Sci.* **2017,** *114* (51), 13374.
94. Niblett, S. P.; Limmer, D. T. Ion Dissociation Dynamics in an Aqueous Premelting Layer. *J. Phys. Chem. B* **2021,** *125* (8), 2174-2181.
95. Hellstern, T. R.; Palm, D. W.; Carter, J.; DeAngelis, A. D.; Horsley, K.; Weinhardt, L.; Yang, W.; Blum, M.; Gaillard, N.; Heske, C.; Jaramillo, T. F. Molybdenum Disulfide Catalytic Coatings via Atomic Layer Deposition for Solar Hydrogen Production from Copper Gallium Diselenide Photocathodes. *ACS Appl. Energy Mat.* **2019,** *2* (2), 1060-1066.
96. Léon, A.; Fiedler, A.; Blum, M.; Benkert, A.; Meyer, F.; Yang, W.; Bär, M.; Scheiba, F.; Ehrenberg, H.; Weinhardt, L.; Heske, C. Valence Electronic Structure of Li2O2, Li2O, Li2CO3,

and LiOH Probed by Soft X-ray Emission Spectroscopy. *J. Phys. Chem. C* **2017,** *121* (10), 5460-5466.
97. Hammer, B.; Hansen, L. B.; Nørskov, J. K. Improved adsorption energetics within density-functional theory using revised Perdew-Burke-Ernzerhof functionals. *Phys. Rev. B* **1999,** *59* (11), 7413-7421.
98. Lynch, M.; Hu, P. A density functional theory study of CO and atomic oxygen chemisorption on Pt(111). *Surf. Sci.* **2000,** *458* (1), 1-14.
99. Feibelman, P. J.; Hammer, B.; Nørskov, J. K.; Wagner, F.; Scheffler, M.; Stumpf, R.; Watwe, R.; Dumesic, J. The CO/Pt(111) Puzzle. *J. Phys. Chem. B* **2001,** *105* (18), 4018-4025.
100. Schimka, L.; Harl, J.; Stroppa, A.; Grüneis, A.; Marsman, M.; Mittendorfer, F.; Kresse, G. Accurate surface and adsorption energies from many-body perturbation theory. *Nature Mat.* **2010,** *9* (9), 741-744.
101. Lininger, C. N.; Gauthier, J. A.; Li, W.-L.; Rossomme, E.; Welborn, V. V.; Lin, Z.; Head-Gordon, T.; Head-Gordon, M.; Bell, A. T. Challenges for density functional theory: calculation of CO adsorption on electrocatalytically relevant metals. *Phys. Chem. Chem. Phys.* **2021,** *23* (15), 9394-9406.
102. Sun, J.; Haunschild, R.; Xiao, B.; Bulik, I. W.; Scuseria, G. E.; Perdew, J. P. Semilocal and hybrid meta-generalized gradient approximations based on the understanding of the kinetic-energy-density dependence. *J. Chem. Phys.* **2013,** *138* (4), 044113-044113.
103. Sun, J.; Remsing, R. C.; Zhang, Y.; Sun, Z.; Ruzsinszky, A.; Peng, H.; Yang, Z.; Paul, A.; Waghmare, U.; Wu, X.; Klein, M. L.; Perdew, J. P. Accurate first-principles structures and energies of diversely bonded systems from an efficient density functional. *Nature Chem.* **2016,** *8* (9), 831-836.
104. Mardirossian, N.; Ruiz Pestana, L.; Womack, J. C.; Skylaris, C.-K.; Head-Gordon, T.; Head-Gordon, M. Use of the rVV10 Nonlocal Correlation Functional in the B97M-V Density Functional: Defining B97M-rV and Related Functionals. *J. Phys. Chem. Lett.* **2017,** *8* (1), 35-40.
105. Cao, X.-M.; Burch, R.; Hardacre, C.; Hu, P. An understanding of chemoselective hydrogenation on crotonaldehyde over Pt(111) in the free energy landscape: The microkinetics study based on first-principles calculations. *Catalysis Today* **2011,** *165* (1), 71-79.
106. Wang, Z.; Liu, X.; Rooney, D. W.; Hu, P. Elucidating the mechanism and active site of the cyclohexanol dehydrogenation on copper-based catalysts: A density functional theory study. *Surf. Sci.* **2015,** *640*, 181-189.
107. Ruiz Pestana, L.; Mardirossian, N.; Head-Gordon, M.; Head-Gordon, T. Ab initio molecular dynamics simulations of liquid water using high quality meta-GGA functionals. *Chem. Sci.* **2017,** *8* (5), 3554-3565.
108. Sebastiani, F.; Bender, T. A.; Pezzotti, S.; Li, W. L.; Schwaab, G.; Bergman, R. G.; Raymond, K. N.; Toste, F. D.; Head-Gordon, T.; Havenith, M. An isolated water droplet in the aqueous solution of a supramolecular tetrahedral cage. *Proc. Natl. Acad. Sci. USA* **2020,** *117* (52), 32954-32961.
109. Novelli, F.; Ruiz Pestana, L.; Bennett, K. C.; Sebastiani, F.; Adams, E. M.; Stavrias, N.; Ockelmann, T.; Colchero, A.; Hoberg, C.; Schwaab, G.; Head-Gordon, T.; Havenith, M. Strong Anisotropy in Liquid Water upon Librational Excitation Using Terahertz Laser Fields. *J. Phys. Chem. B* **2020,** *124* (24), 4989-5001.

110. Morhart, T. A.; Read, S. T.; Wells, G.; Jacobs, M.; Rosendahl, S. M.; Achenbach, S.; Burgess, I. J. Micromachined multigroove silicon ATR FT-IR internal reflection elements for chemical imaging of microfluidic devices. *Anal. Meth.* **2019,** *11* (45), 5776-5783.
111. Eriksson, M.; van der Veen, J. F.; Quitmann, C. Diffraction-limited storage rings - a window to the science of tomorrow. *J Synch. Rad.* **2014,** *21* (Pt 5), 837-42.
112. *ALS-U: Solving Scientific Challenges with Coherent Soft X-Rays*; Lawrence Berkeley National Laboratory: Berkeley, 2017.
113. Perakis, F.; Amann-Winkel, K.; Lehmkuhler, F.; Sprung, M.; Mariedahl, D.; Sellberg, J. A.; Pathak, H.; Spah, A.; Cavalca, F.; Schlesinger, D.; Ricci, A.; Jain, A.; Massani, B.; Aubree, F.; Benmore, C. J.; Loerting, T.; Grubel, G.; Pettersson, L. G. M.; Nilsson, A. Diffusive dynamics during the high-to-low density transition in amorphous ice. *Proc. Natl. Acad. Sci. USA* **2017,** *114* (31), 8193-8198.
114. Niskanen, J.; Fondell, M.; Sahle, C. J.; Eckert, S.; Jay, R. M.; Gilmore, K.; Pietzsch, A.; Dantz, M.; Lu, X. Y.; McNally, D. E.; Schmitt, T.; da Cruz, V. V.; Kimberg, V.; Gel'mukhanov, F.; Fohlisch, A. Compatibility of quantitative X-ray spectroscopy with continuous distribution models of water at ambient conditions. *Proc. Natl. Acad. Sci. USA* **2019,** *116* (10), 4058-4063.
115. Vaz da Cruz, V.; Gel'mukhanov, F.; Eckert, S.; Iannuzzi, M.; Ertan, E.; Pietzsch, A.; Couto, R. C.; Niskanen, J.; Fondell, M.; Dantz, M.; Schmitt, T.; Lu, X.; McNally, D.; Jay, R. M.; Kimberg, V.; Föhlisch, A.; Odelius, M. Probing hydrogen bond strength in liquid water by resonant inelastic X-ray scattering. *Nature Comm.* **2019,** *10* (1), 1013.
116. Lu, W.; Zhang, E.; Amarasinghe, C.; Kostko, O.; Ahmed, M. Probing Self-Assembly in Arginine-Oleic Acid Solutions with Terahertz Spectroscopy and X-ray Scattering. *J. Phys. Chem. Lett.* **2020,** *11* (21), 9507-9514.
117. Qian, J.; Crumlin, E. J. Digital Twin: A Theorist's Playground for APXPS and Surface Science. In *Am. Phys. Soc.*, Virtual, 2021.
118. Haghighatlari, M.; Li, J.; Heidar-Zadeh, F.; Liu, Y.; Guan, X.; Head-Gordon, T. Learning to Make Chemical Predictions: The Interplay of Feature Representation, Data, and Machine Learning Methods. *Chem* **2020,** *6* (7), 1527-1542.
119. Blau, S. M.; Patel, H. D.; Spotte-Smith, E. W. C.; Xie, X.; Dwaraknath, S.; Persson, K. A. A chemically consistent graph architecture for massive reaction networks applied to solid-electrolyte interphase formation. *Chem. Sci.* **2021,** *12* (13), 4931-4939.
120. Schile, A. J.; Limmer, D. T. Studying rare nonadiabatic dynamics with transition path sampling quantum jump trajectories. *J. Chem. Phys.* **2018,** *149* (21), 214109.
121. Schile, A. J.; Limmer, D. T. Simulating conical intersection dynamics in the condensed phase with hybrid quantum master equations. *J. Chem. Phys.* **2019,** *151* (1), 014106.
122. Yunger Halpern, N.; Limmer, D. T. Fundamental limitations on photoisomerization from thermodynamic resource theories. *Phys. Rev. A* **2020,** *101* (4), 042116.
123. Das, A.; Limmer, D. T. Variational design principles for nonequilibrium colloidal assembly. *J. Chem. Phys.* **2021,** *154* (1), 014107.
124. Das, A.; Limmer, D. T. Variational control forces for enhanced sampling of nonequilibrium molecular dynamics simulations. *J. Chem. Phys.* **2019,** *151* (24), 244123.